

Electroexcitation of the $\Delta(1232)_{\frac{3}{2}}^{+}$ and $\Delta(1600)_{\frac{3}{2}}^{+}$ in a light-front relativistic quark model

I.G. Aznauryan^{1,2} and V.D. Burkert¹

¹ *Thomas Jefferson National Accelerator Facility, Newport News, Virginia 23606, USA*

² *Yerevan Physics Institute, 375036 Yerevan, Armenia*

The magnetic-dipole form factor and the ratios R_{EM} and R_{SM} for the $\gamma^*N \rightarrow \Delta(1232)_{\frac{3}{2}}^{+}$ transition are predicted within light-front relativistic quark model up to photon virtuality $Q^2 = 12 \text{ GeV}^2$. We also predict the helicity amplitudes of the $\gamma^*N \rightarrow \Delta(1600)_{\frac{3}{2}}^{+}$ transition assuming the $\Delta(1600)_{\frac{3}{2}}^{+}$ is the first radial excitation of the ground state $\Delta(1232)_{\frac{3}{2}}^{+}$.

PACS numbers: 12.39.Ki, 13.40.Gp, 13.40.Hq, 14.20.Gk

I. INTRODUCTION

One of the longstanding and intriguing problems of hadron physics is the identification of the states that can be assigned as the first radial excitations of the nucleon and $\Delta(1232)_{\frac{3}{2}}^{+}$. It is well recognized that the crucial role in the identification of the Roper resonance $N(1440)_{\frac{1}{2}}^{+}$ as a predominantly first radial excitation of the three-quark ($3q$) ground state belongs to the measurements by the CLAS collaboration [1–6] that resulted in the determination of the electrocouplings of this resonance with the proton in a wide range of $Q^2 = 0.3 - 4.2 \text{ GeV}^2$. Comparison of the $\gamma^*p \rightarrow N(1440)_{\frac{1}{2}}^{+}$ transition amplitudes extracted from these data [7, 8] with the predictions of the LF relativistic quark models (LF RQM) [9, 10] provided strong evidence for the $N(1440)_{\frac{1}{2}}^{+}$ as a member of the multiplet $[56, 0^+]_r$, with additional non-3-quark contributions needed to describe the low Q^2 behavior of the amplitudes.

Our goal in this paper is computation of the $\gamma^*N \rightarrow \Delta(1600)_{\frac{3}{2}}^{+}$ transition amplitudes in the LF RQM. Comparison of the results obtained in the quark model with the amplitudes that are expected to be extracted from experimental data will provide important test for the commonly expected assignment of the $\Delta(1600)_{\frac{3}{2}}^{+}$ as the first radial excitation of the $\Delta(1232)_{\frac{3}{2}}^{+}$. Very recently, the CLAS data on the differential cross sections of exclusive process $ep \rightarrow e\pi^+n$ were reported in the range of $Q^2 = 1.8 - 4 \text{ GeV}^2$, and the invariant mass range of the π^+n final state $W = 1.6 - 2.0 \text{ GeV}$ [11]. These data combined with the earlier CLAS data [6] on the cross sections and longitudinally polarized beam asymmetries for this reaction in the lower mass range $W = 1.15 - 1.69 \text{ GeV}$ and at close values of Q^2 allowed the extraction of the electroexcitation amplitudes of the resonances $N(1675)_{\frac{5}{2}}^{-}$, $N(1680)_{\frac{5}{2}}^{+}$, and $N(1710)_{\frac{1}{2}}^{+}$ in the third resonance region. The isotopic pairs of the resonances from this region: $\Delta(1600)_{\frac{3}{2}}^{+}$ and $N(1720)_{\frac{3}{2}}^{+}$, $\Delta(1620)_{\frac{1}{2}}^{-}$ and $N(1650)_{\frac{1}{2}}^{-}$, and $\Delta(1700)_{\frac{3}{2}}^{-}$ and $N(1700)_{\frac{3}{2}}^{-}$, could not be separated from each other using data from a single isospin channel. Currently new data are in preparation

by the CLAS collaboration for the $ep \rightarrow ep\pi^0$ process in the same kinematics region as the data in the $ep \rightarrow en\pi^+$ channel [6, 11], as well as at lower Q^2 . The two-channel analysis will allow the extraction of the electroexcitation amplitudes of all resonances from the third resonance region including the $\Delta(1600)_{\frac{3}{2}}^{+}$.

The approach we use is based on the LF dynamics and is formulated in Refs. [12, 13]. In numerous applications (see Refs. [10, 14] and references therein), this approach was utilized for the investigation of nucleon form factors and electroexcitation of nucleon resonances.

In this work we study the electroexcitation of the $\Delta(1600)_{\frac{3}{2}}^{+}$ in parallel with that of the $\Delta(1232)_{\frac{3}{2}}^{+}$, where we complement the results obtained earlier in Ref. [14] by computing all three form factors that describe the transition $\gamma^*N \rightarrow \Delta(1232)_{\frac{3}{2}}^{+}$. In Refs. [15, 16] it was shown that there are difficulties in the utilization of the LF approaches for hadrons with spin $J \geq 1$. In the approach of Ref. [13], these difficulties limit the number of transition amplitudes that can be investigated for the $\Delta(1232)_{\frac{3}{2}}^{+}$ and $\Delta(1600)_{\frac{3}{2}}^{+}$. Reliable results can be obtained only for two of the three transition form factors. They are based on the utilization of longitudinal components of the electromagnetic current $J_{em}^{0,z}$. For the $\Delta(1232)_{\frac{3}{2}}^{+}$, the results obtained for two transition form factors have been presented in Ref. [14]. In the present work, we complement these results by calculating the third transition form factor using $J_{em}^x + iJ_{em}^y$. As was shown in Ref. [13], these results are less reliable, as the matrix elements of transverse components of the electromagnetic current can contain contributions that violate impulse approximation, i.e. contributions of diagrams containing vertices like $\gamma^* \rightarrow q\bar{q}$. Similar problem exists in the LF RQM of Refs. [9, 16], where the requirement of rotational covariance can not be satisfied without introducing two- and three-body current operators. For this reason, the results for the electroexcitation amplitudes for the resonances with spins $J = \frac{3}{2}$ are presented in Ref. [9] along with curves which show the uncertainty that can be caused by the violation of the rotational covariance. When presenting our results we also demonstrate the uncertainty that can arise due to the inclusion of the transverse compo-

nents of the electromagnetic current.

An important aspect in the comparison of the transition amplitudes obtained in theoretical approaches with the amplitudes extracted from experimental data is their sign (see, for example, Ref. [17]). The results on the $\gamma^*N \rightarrow N^*$ transition amplitudes extracted from experimental data contain an additional sign related to the vertex of the resonance coupling to the final state hadrons. In the electroproduction of pions on nucleons this is the relative sign between the πNN^* and πNN vertices. For the Roper resonance, this sign was found in Refs. [9] and [10] using, respectively, the 3P_0 model and the approach based on PCAC in the way suggested in Ref. [18]. The results obtained in both approaches are consistent with each other. In Sec. II, we determine the relative signs of the vertices πNN , $\pi N\Delta(1232)$, and $\pi N\Delta(1600)$ using the approach based on PCAC.

Our goals and the ranges of Q^2 , where we make predictions, for the resonances $\Delta(1232)_{\frac{3}{2}^+}$ and $\Delta(1600)_{\frac{3}{2}^+}$ are different. For the $\Delta(1600)_{\frac{3}{2}^+}$, we make predictions that are of interest to reveal the nature of this resonance using the existing and future CLAS data at $Q^2 < 4 \text{ GeV}^2$. For the $\Delta(1232)_{\frac{3}{2}^+}$, our goal is to make predictions up to 12 GeV^2 . These results will be important for the interpretation of future data on $\gamma^*p \rightarrow \Delta(1232)_{\frac{3}{2}^+}$ that are expected with the Jefferson Lab 12 GeV upgrade.

In Sec. II we present the LF RQM formalism to compute the $\gamma^*N \rightarrow \Delta$ transition amplitudes. The results for both resonances are presented and discussed in Sec. III and summarized in Sec. IV.

II. THE $\gamma^*N \rightarrow \Delta$ TRANSITION AMPLITUDES IN LF RQM

The $\gamma^*N \rightarrow \Delta(1232)_{\frac{3}{2}^+}$ and $\gamma^*N \rightarrow \Delta(1600)_{\frac{3}{2}^+}$ amplitudes have been evaluated within the approach of Ref. [13] where the LF RQM is formulated in the infinite momentum frame (IMF). The IMF is chosen in such a way, that the initial hadron moves along the z -axis with the momentum $\mathbf{P} \rightarrow \infty$, the virtual photon momentum is $\mathbf{k}^\mu = \left(\frac{M^2 - m^2 - \mathbf{Q}_\perp^2}{4P}, \mathbf{Q}_\perp, -\frac{M^2 - m^2 - \mathbf{Q}_\perp^2}{4P} \right)$, the final hadron momentum is $\mathbf{P}' = \mathbf{P} + \mathbf{k}$, and $\mathbf{Q}^2 \equiv -\mathbf{k}^2 = \mathbf{Q}_\perp^2$; m and M are masses of the nucleon and Δ , respectively. In this frame, the matrix elements of the electromagnetic current for the $\gamma^*N \rightarrow \Delta$ transition have the form:

$$\begin{aligned} & \langle \Delta, S'_z | J_{em}^\mu | N, S_z \rangle |_{\mathbf{P} \rightarrow \infty} \\ & = 3eQ_a \int \Psi'^+(\mathbf{p}'_a, \mathbf{p}'_b, \mathbf{p}'_c) \Gamma_a^\mu \Psi(\mathbf{p}_a, \mathbf{p}_b, \mathbf{p}_c) d\Gamma, \end{aligned} \quad (1)$$

where S_z and S'_z are the projections of the hadron spins on the z -direction. In Eq. (1), it is supposed that the photon interacts with quark a (the quarks in hadrons are denoted by a, b, c), Q_a is the charge of this quark in units of e ($e^2/4\pi = 1/137$); Ψ and Ψ' are wave functions in the vertices $N(\Delta) \leftrightarrow 3q$; \mathbf{p}_i and \mathbf{p}'_i ($i = a, b, c$) are the

quark momenta in IMF; $d\Gamma$ is the phase space volume; Γ_a^μ corresponds to the vertex of the quark interaction with the photon:

$$x_a \Gamma_a^x = 2p_{ax} + Q_x + iQ_y \sigma_z^{(a)}, \quad (2)$$

$$x_a \Gamma_a^y = 2p_{ay} + Q_y - iQ_x \sigma_z^{(a)}, \quad (3)$$

$$\Gamma_a^0 = \Gamma_a^z = 2P, \quad (4)$$

where x_a is the fraction of the initial hadron momentum carried by the quark.

Let \mathbf{q}_i ($i = a, b, c$) be the three-momenta of initial quarks in their c.m.s.: $\mathbf{q}_a + \mathbf{q}_b + \mathbf{q}_c = 0$. The sets of the quark three-momenta in the IMF and in the c.m.s. of the quarks are related as follows:

$$\mathbf{p}_i = x_i \mathbf{P} + \mathbf{q}_{i\perp}, \quad \sum_i x_i = 1. \quad (5)$$

According to results of Ref. [13], the wave function Ψ is related to the wave function in the c.m.s. of quarks through Melosh matrices [19]:

$$\Psi = U^+(\mathbf{p}_a)U^+(\mathbf{p}_b)U^+(\mathbf{p}_c)\Psi_{fss}\Phi(\mathbf{q}_a, \mathbf{q}_b, \mathbf{q}_c). \quad (6)$$

Here we have separated the flavor-spin-space (Ψ_{fss}) and spatial (Φ) parts of the c.m.s. wave function. The Melosh matrices are

$$U(\mathbf{p}_i) = \frac{m_q + M_0 x_i + i\epsilon_{lm}\sigma_l \mathbf{q}_{im}}{\sqrt{(m_q + M_0 x_i)^2 + \mathbf{q}_{i\perp}^2}}, \quad (7)$$

where m_q is the quark mass and M_0 is invariant mass of the system of initial quarks:

$$M_0^2 = \left(\sum_i \mathbf{p}_i \right)^2 = \sum_i \frac{\mathbf{q}_{i\perp}^2 + m_q^2}{x_i}. \quad (8)$$

In the c.m.s. of quarks:

$$M_0 = \sum_i \omega_i, \quad \omega_i = \sqrt{m_q^2 + \mathbf{q}_i^2}, \quad \mathbf{q}_{iz} + \omega_i = M_0 x_i. \quad (9)$$

For the final state quarks, the quantities defined by Eqs. (5-9) are expressed through \mathbf{p}'_i , \mathbf{q}'_i , and M'_0 . The phase space volume in Eq. (1) has the form:

$$d\Gamma = (2\pi)^{-6} \frac{d\mathbf{q}_{b\perp} d\mathbf{q}_{c\perp} dx_b dx_c}{4x_a x_b x_c}. \quad (10)$$

To study sensitivity to the form of the quark wave function, we employed two forms of the spatial wave function:

$$\Phi_{N(\Delta)}^{(1)} = N_{N(\Delta)}^{(1)} \exp(-M_0^2/6\alpha_1^2), \quad (11)$$

$$\Phi_{\Delta_r}^{(1)} = N_{\Delta_r}^{(1)} (\beta_1^2 - M_0^2) \exp(-M_0^2/6\alpha_1^2) \quad (12)$$

and

$$\Phi_{N(\Delta)}^{(2)} = N_{N(\Delta)}^{(2)} \exp [-(\mathbf{q}_a^2 + \mathbf{q}_b^2 + \mathbf{q}_c^2)/2\alpha_2^2], \quad (13)$$

$$\Phi_{\Delta_r}^{(2)} = N_{\Delta_r}^{(2)} [\beta_2^2 - (\mathbf{q}_a^2 + \mathbf{q}_b^2 + \mathbf{q}_c^2)] \exp [-(\mathbf{q}_a^2 + \mathbf{q}_b^2 + \mathbf{q}_c^2)/2\alpha_2^2], \quad (14)$$

that were used, respectively, in Refs. [12, 13] and [9]. The parameters N and β are determined by the conditions:

$$\int \Phi_{N(\Delta, \Delta_r)}^2 d\Gamma = 1, \quad \int \Phi_{N(\Delta)} \Phi_{\Delta_r} d\Gamma = 0. \quad (15)$$

To distinguish between ground state $\Delta(1232)$ and the $\Delta(1600)$, considered as the member of the multiplet $[56, 0^+]_r$, we have used in Eqs. (11-15) notations Δ and Δ_r .

Other parameters of the model, namely, the quark mass m_q and the oscillator parameter α , were found in Ref. [14] from the description of nucleon form factors up to $Q^2 = 16 \text{ GeV}^2$:

$$\alpha_1 = 0.37 \text{ GeV}, \quad \alpha_2 = 0.41 \text{ GeV}, \quad (16)$$

$$m_q^{(1)}(Q^2) = \frac{0.22 \text{ GeV}}{1 + Q^2/56 \text{ GeV}^2}, \quad (17)$$

$$m_q^{(2)}(Q^2) = \frac{0.22 \text{ GeV}}{1 + Q^2/18 \text{ GeV}^2}. \quad (18)$$

The Q^2 -dependence of the constituent quark mass (17,18) is in qualitative agreement with the QCD lattice calculations and Dyson-Schwinger equations [20–22], where the running quark mass is generated dynamically. The parameters (16) and the parameterizations (17,18) have been used in the present calculations. For both resonances, the results for the transition amplitudes obtained with the wave functions (11,12) and (13,14) turned out very close to each other.

Electroexcitation of the states with $J^P = \frac{3}{2}^+$ on the nucleon is described by three form factors $G_1(Q^2)$, $G_2(Q^2)$, and $G_3(Q^2)$, which we define according to Refs. [17, 23] in the following way:

$$\langle \Delta, J^P = \frac{3}{2}^+ | J_{em}^\mu | N \rangle \equiv e \bar{u}_\nu(P') \gamma_5 \Gamma^{\nu\mu} u(P), \quad (19)$$

$$\Gamma^{\nu\mu}(Q^2) = G_1 \mathcal{H}_1^{\nu\mu} + G_2 \mathcal{H}_2^{\nu\mu} + G_3 \mathcal{H}_3^{\nu\mu}, \quad (20)$$

$$\mathcal{H}_1^{\nu\mu} = \not{k} g^{\nu\mu} - k^\nu \gamma^\mu, \quad (21)$$

$$\mathcal{H}_2^{\nu\mu} = k^\nu P'^\mu - (kP') g^{\nu\mu}, \quad (22)$$

$$\mathcal{H}_3^{\nu\mu} = k^\nu k^\mu - k^2 g^{\nu\mu}, \quad (23)$$

where $u(P)$ and $u_\nu(P')$ are, respectively, the Dirac and Rarita-Schwinger spinors. These form factors have been found through the matrix elements (1) using the relations:

$$\frac{1}{2P} \langle \Delta, \frac{3}{2} | J_{em}^{0,z} | N, \frac{1}{2} \rangle |_{P \rightarrow \infty} = -\frac{Q}{\sqrt{2}} \left[G_1(Q^2) + \frac{M-m}{2} G_2(Q^2) \right], \quad (24)$$

$$\frac{1}{2P} \langle \Delta, \frac{3}{2} | J_{em}^{0,z} | N, -\frac{1}{2} \rangle |_{P \rightarrow \infty} = \frac{Q^2}{2\sqrt{2}} G_2(Q^2), \quad (25)$$

$$\langle \Delta, \frac{3}{2} | J_{em}^x + i J_{em}^y | N, -\frac{1}{2} \rangle |_{P \rightarrow \infty} = \frac{Q^3}{\sqrt{2}} G_3(Q^2). \quad (26)$$

The relations between form factors $G_1(Q^2)$, $G_2(Q^2)$, and $G_3(Q^2)$ and the $\gamma^* N \rightarrow \Delta(\frac{3}{2}^+)$ helicity amplitudes and the Jones-Scadron form factors $G_M(Q^2)$, $G_E(Q^2)$, and $G_C(Q^2)$ [24] are given in the Appendix.

In the approach based on PCAC, the relative signs of the πNN , $\pi N\Delta(1232)$, and $\pi N\Delta(1600)$ vertices are determined according to Refs. [10, 15] by the relative signs of the following expressions:

$$I_{NA} \equiv \int \frac{(m_q + M_0 x_a)^2 - \mathbf{q}_{a\perp}^2}{(m_q + M_0 x_a)^2 + \mathbf{q}_{a\perp}^2} \Phi_N(M_0^2) \Phi_A(M_0^2) d\Gamma, \quad (27)$$

where A denotes the states N , $\Delta(1232)$, and $\Delta(1600)$. Numerical calculation of I_{NN} , $I_{N\Delta(1232)}$, and $I_{N\Delta(1600)}$ with the wave functions (11-14) gives positive relative signs for the πNN , $\pi N\Delta(1232)$, and $\pi N\Delta(1600)$ vertices.

III. RESULTS

A. The $\Delta(1232)\frac{3}{2}^+$ resonance

We present the results for the $\Delta(1232)\frac{3}{2}^+$ in terms of the $\gamma^* p \rightarrow \Delta(1232)\frac{3}{2}^+$ magnetic-dipole transition form factor in the Ash convention [25] (Fig. 1) and the ratios $R_{EM} \equiv ImE_{1+}^{3/2}/ImM_{1+}^{3/2}$ and $R_{SM} \equiv ImS_{1+}^{3/2}/ImM_{1+}^{3/2}$ (Fig. 2). These observables are commonly used to present the results on the $\Delta(1232)\frac{3}{2}^+$ extracted from experimental data on the electroproduction of pions on nucleons. The $\gamma^* p \rightarrow \Delta(1232)\frac{3}{2}^+$ magnetic-dipole form factor in the Ash convention is related to the Jones-Scadron form factor defined in the Appendix as follows:

$$G_{M,Ash}(Q^2) = \frac{G_M(Q^2)}{\sqrt{1 + \frac{Q^2}{(M+m)^2}}}. \quad (28)$$

The ratios R_{EM} and R_{SM} are related to the Jones-Scadron form factors by:

$$R_{EM} = -\frac{G_E}{G_M}, \quad R_{SM} = -\frac{G_C}{G_M} \frac{K}{2m}, \quad (29)$$

where K is the virtual photon 3-momentum in the c.m.s. of the reaction $\gamma^* N \rightarrow \pi N$:

$$K \equiv \frac{\sqrt{Q_+ Q_-}}{2M}, \quad Q_{\pm} \equiv (M \pm m)^2 + Q^2. \quad (30)$$

As it was mentioned in the Introduction, in the approach that we utilize [13], the results are reliable that are obtained through longitudinal components of the electromagnetic current $J_{em}^{0,z}$, i.e. the results for the form factors $G_1(Q^2)$ and $G_2(Q^2)$ (24,25). These results have been presented and discussed in Ref. [14]. In this paper, we complement the results for $G_1(Q^2)$ and $G_2(Q^2)$ by calculating the third transition form factor $G_3(Q^2)$ using $J_{em}^x + iJ_{em}^y$ (26). This allows us to present the predictions in a more convenient way in terms of $G_{M,Ash}$ and R_{EM} and R_{SM} . In order to demonstrate the uncertainty that can arise due to inclusion of the transverse components of the electromagnetic current, we also present in Figs. 1,2 results that correspond to the values of $G_3(Q^2)$ taken with $\pm 50\%$ deviation from the values obtained using the relation (26).

It is known that at relatively small Q^2 , nearly massless pions generate pion-loop contributions that significantly alter three-quark contribution to $\gamma^* p \rightarrow \Delta(1232)_{\frac{3}{2}^+}$ [39–41]. It is expected that the corresponding hadronic component, including contributions from other mesons, will be rapidly losing strength with increasing Q^2 . From the description of the data on pion electroproduction on proton within dynamical reaction model [37, 38], it follows that the contribution associated with the meson-baryon contribution to $\gamma^* p \rightarrow \Delta(1232)_{\frac{3}{2}^+}$ (dashed-dotted curve in Fig. 1) can be neglected above $Q^2 = 4 \text{ GeV}^2$. Therefore, the weight of the $3q$ contribution to the $\Delta(1232)_{\frac{3}{2}^+}$:

$$|\Delta(1232)\rangle = c_{\Delta}|3q\rangle + \dots, \quad (31)$$

was found in Ref. [14] from the description of the form factors $G_1(Q^2)$ and $G_2(Q^2)$ at $Q^2 > 4 \text{ GeV}^2$:

$$c_{\Delta} = 0.53 \pm 0.04. \quad (32)$$

The uncertainty of c_{Δ} is caused mainly by the systematic uncertainties of the data on $G_{M,Ash}(Q^2)$ at these Q^2 . We have used the value of c_{Δ} from Eq. (32) to find the three-quark contributions to $G_{M,Ash}(Q^2)$ and R_{EM} and R_{SM} , that are presented in Figs. 1,2.

From the discussion above, it follows that at $Q^2 < 4 \text{ GeV}^2$, meson-baryon contributions alter the three-quark contribution to $\gamma^* p \rightarrow \Delta(1232)_{\frac{3}{2}^+}$ [37–41]. With this, for the magnetic-dipole form factor, these contributions definitely result in better agreement with experiment. Above $4 - 5 \text{ GeV}^2$, we expect that the $\gamma^* p \rightarrow \Delta(1232)_{\frac{3}{2}^+}$ transition will be determined by

the three-quark contribution only. Therefore, we consider our results at these Q^2 as predictions for the $\gamma^* p \rightarrow \Delta(1232)_{\frac{3}{2}^+}$ transition amplitudes obtained within nonperturbative approach.

For the form factor $G_{M,Ash}(Q^2)$, the spread of our results caused by uncertainties in the form factor $G_3(Q^2)$ is insignificant, and we have definite predictions up to 12 GeV^2 . According to these predictions, above 5 GeV^2 the behaviour of the ratio $G_{M,Ash}(Q^2)/G_D(Q^2)$ becomes more flat in comparison with that at lower Q^2 . The similar Q^2 -dependence is observed for the proton magnetic form factor [42]. For the Jones-Scadron magnetic-dipole form factor $G_M(Q^2)$ and the proton magnetic form factor $G_{M,p}(Q^2)$, the Q^2 -dependences at $Q^2 = 5 - 12 \text{ GeV}^2$ practically coincide.

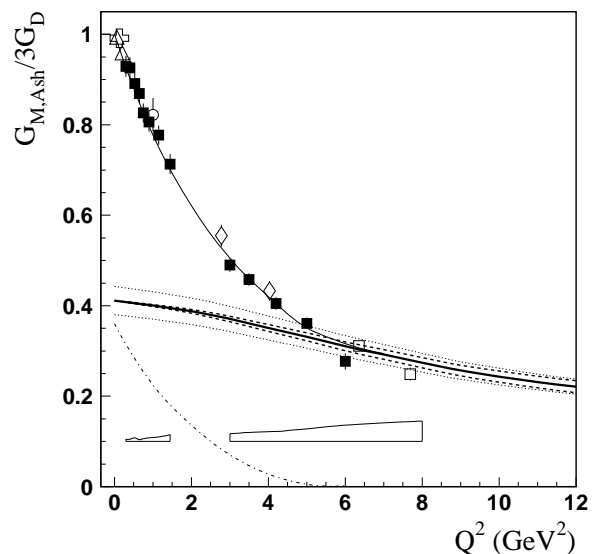


FIG. 1: The form factor $G_{M,Ash}(Q^2)$ for the $\gamma^* p \rightarrow \Delta(1232)_{\frac{3}{2}^+}$ transition relative to $3G_D$: $G_D(Q^2) = 1/(1 + \frac{Q^2}{0.71 \text{ GeV}^2})$. The full boxes are the CLAS data extracted in the analysis of Ref. [8], the open boxes correspond to the data from Ref. [26]. The bands show the model uncertainties of these data [8, 17]. The thin solid curve is the result of the global analysis of the Mainz group [27]. The results from other experiments are: open triangles [28–30], open cross [31–33], open rhombuses [34], and open circle [35, 36]. The thick solid curve presents our results; the dashed curves are our results corresponding to $\pm 50\%$ deviation of $G_3(Q^2)$ from the values obtained using the relation (26); the dotted curves show the uncertainty of our results (given by the solid curve) that is caused by the uncertainty of c_{Δ} (32). The dashed-dotted curve is meson-baryon contribution from Refs. [37, 38].

For the ratios R_{EM} and R_{SM} , the spread of predictions grows from 6 to 10%, when Q^2 is increasing from 5 to 12 GeV^2 . Nevertheless, for the ratio R_{SM} one can definitely conclude, that according to our predictions R_{SM} will continue to grow and within the $Q^2 = 12 \text{ GeV}^2$ limit will not reach the value predicted in pQCD, i.e. $R_{SM} \rightarrow \text{const}$ with undefined sign and magnitude. On

the other hand, in holographic QCD in the large N_c limit the R_{SM} ratio is predicted at the specific asymptotic value: $R_{SM} \rightarrow -100\%$ [43]. The data show the correct trend, but are projected to reach only 40 to 50% of that value at $Q^2 \leq 12 \text{ GeV}^2$.

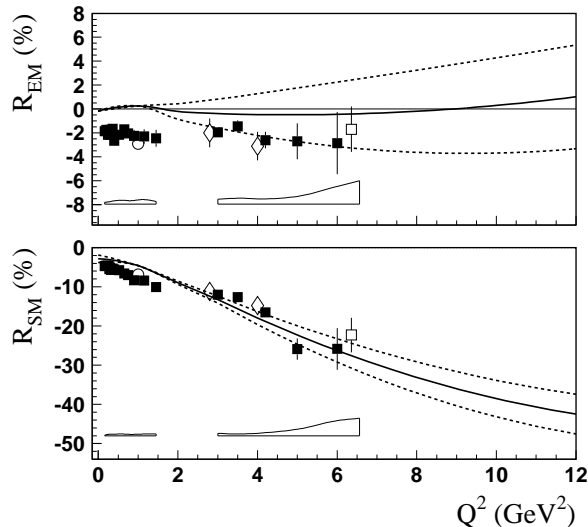


FIG. 2: The ratios R_{EM} , R_{SM} for the $\gamma^*p \rightarrow \Delta(1232)_{\frac{3}{2}}^+$ transition. The legend for experimental data and thick solid and dashed curves is as for Fig. 1.

B. The $\Delta(1600)_{\frac{3}{2}}^+$ resonance

The results for the resonance $\Delta(1600)_{\frac{3}{2}}^+$ are presented in Fig. 3 in terms of the $\gamma^*p \rightarrow \Delta(1600)_{\frac{3}{2}}^+$ helicity amplitudes. The predictions of the LF RQM approach from Ref. [9] are also shown. The common sign of the amplitudes has been found in our approach and in Ref. [9] due to additional computation of the relative signs of the πNN , $\pi N\Delta(1232)$, and $\pi N\Delta(1600)$ vertices using different approaches.

In Section I we have discussed the difficulties in the utilization of the LF approach for hadrons with spin $J \geq 1$. In the approach of Ref. [9] the uncertainty that can be caused by these difficulties for the $\Delta(1600)_{\frac{3}{2}}^+$ nearly coincides with the longitudinal helicity amplitude $S_{1/2}$. In our approach these uncertainties are presented by dashed curves that correspond to the results obtained with the values of $G_3(Q^2)$ taken with $\pm 50\%$ deviation from the values obtained using the relation (26). From the presented results we conclude that independently of uncertainties, both approaches give close pre-

dictions for the transverse helicity amplitudes: these amplitudes, being negative at $Q^2 = 0$, change their signs at $Q^2 = 0.2 - 0.3 \text{ GeV}^2$ and become positive. With this, the values of transverse amplitudes at $Q^2 = 0$ are in good agreement with the RPP estimates [44]. As in the case of the Roper resonance, these features will be crucial for conclusions on the nature of the resonance $\Delta(1600)_{\frac{3}{2}}^+$ that will be obtained from the comparison with the future data on the $\gamma^*p \rightarrow \Delta(1600)_{\frac{3}{2}}^+$ helicity amplitudes.

IV. SUMMARY

We have employed the LF RQM to evaluate the quark core contributions to the transitions $\gamma^*N \rightarrow \Delta(1232)_{\frac{3}{2}}^+$ and $\gamma^*N \rightarrow \Delta(1600)_{\frac{3}{2}}^+$. Our previous evaluation of the 3-quark core contribution to the $\Delta(1232)_{\frac{3}{2}}^+$ based on the $\gamma^*N \rightarrow \Delta(1232)_{\frac{3}{2}}^+$ data up to $Q^2 = 7.5 \text{ GeV}^2$ allowed us to make projections into unmeasured territory of $Q^2 \leq 12 \text{ GeV}^2$. This region may be covered in upcoming measurements with CLAS12 at the Jefferson Lab 12 GeV upgrade. The projections are made for the magnetic-dipole form factor and electric and scalar quadrupole ratios $R_{EM}(Q^2)$ and $R_{SM}(Q^2)$. Predictions for the 3 electrocoupling amplitudes are also made for the $\Delta(1600)_{\frac{3}{2}}^+$ in the range $Q^2 \leq 5 \text{ GeV}^2$ assuming this state is the first radial excitation of the $\Delta(1232)_{\frac{3}{2}}^+$. The predicted very rapid transition from large negative values at the real photon point to large positive values with maxima near $Q^2 = 1 - 2 \text{ GeV}^2$, and a slow falloff with Q^2 for the two transverse amplitudes, should be readily accessible to experimental exploration.

V. ACKNOWLEDGMENTS

This work was supported by the US Department of Energy under contract DE-AC05-06OR23177 and the National Science Foundation and State Committee of Science of Republic of Armenia, Grant-13-1C023.

VI. APPENDIX. THE RELATIONS BETWEEN THE $\gamma^*N \rightarrow \Delta(\frac{3}{2}^+)$ FORM FACTORS AND HELICITY AMPLITUDES

The relations between the form factors $G_1(Q^2)$, $G_2(Q^2)$, and $G_3(Q^2)$ defined by Eqs. (19-23) and the $\gamma^*N \rightarrow \Delta(\frac{3}{2}^+)$ helicity amplitudes are following [17, 23]:

$$A_{1/2} = h_3 X, \quad A_{3/2} = \sqrt{3} h_2 X, \quad S_{1/2} = h_1 \frac{K}{\sqrt{2}M} X, \quad (\text{A1})$$

where

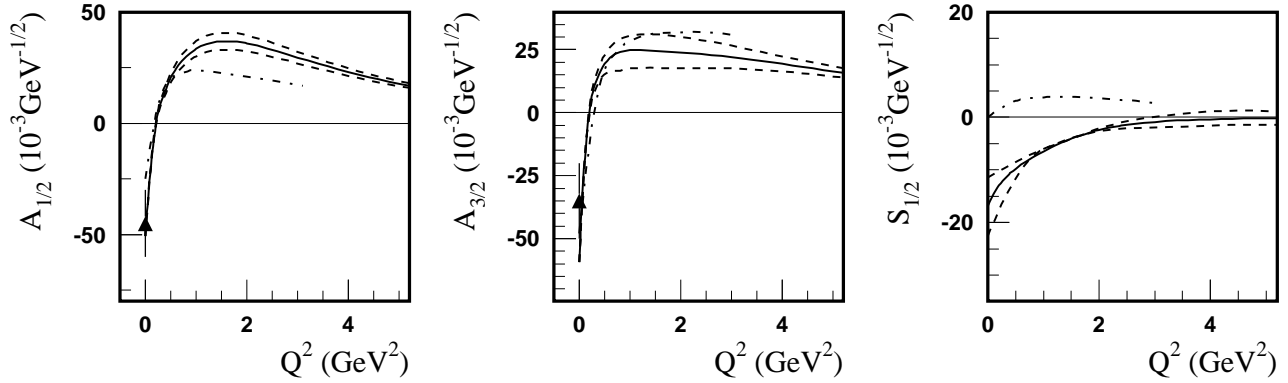


FIG. 3: Helicity amplitudes for the $\gamma^* p \rightarrow \Delta(1600)_{\frac{3}{2}^+}$ transition. The full triangles at $Q^2 = 0$ are the RPP estimates [44]. The thick solid curve presents our results. The legend for dashed curves is as for Fig. 1. The dashed-dotted curves present the predictions from Ref. [9].

$$h_1(Q^2) = 4MG_1(Q^2) + 4M^2G_2(Q^2) + 2(M^2 - m^2 - Q^2)G_3(Q^2), \quad (\text{A2})$$

$$h_2(Q^2) = -2(M+m)G_1(Q^2) - (M^2 - m^2 - Q^2)G_2(Q^2) + 2Q^2G_3(Q^2), \quad (\text{A3})$$

$$h_3(Q^2) = -\frac{2}{M}[Q^2 + m(M+m)]G_1(Q^2) + (M^2 - m^2 - Q^2)G_2(Q^2) - 2Q^2G_3(Q^2), \quad (\text{A4})$$

$$X \equiv e\sqrt{\frac{Q_-}{48m(M^2 - m^2)}}. \quad (\text{A5})$$

and $G_C(Q^2)$ [24] are defined by:

$$G_M(Q^2) = -Y(\sqrt{3}A_{3/2} + A_{1/2}), \quad (\text{A6})$$

$$G_E(Q^2) = -Y(A_{3/2}/\sqrt{3} - A_{1/2}), \quad (\text{A7})$$

$$G_C(Q^2) = 2\sqrt{2}\frac{M}{K}YS_{1/2}, \quad (\text{A8})$$

$$Y \equiv \frac{m}{e(M+m)}\sqrt{\frac{2m(M^2 - m^2)}{Q_-}}. \quad (\text{A9})$$

The Jones-Scadron form factors $G_M(Q^2)$, $G_E(Q^2)$,

-
- [1] K. Joo et al., CLAS Collaboration, Phys. Rev. Lett. **88**, 122001 (2002).
[2] K. Joo et al., CLAS Collaboration, Phys. Rev. C **68**, 032201 (2003).
[3] K. Joo et al., CLAS Collaboration, Phys. Rev. C **70**, 042201 (2004).
[4] H. Egiyan et al., CLAS Collaboration, Phys. Rev. C **73**, 025204 (2006).
[5] A. Biselli et al., CLAS Collaboration, Phys. Rev. C **78**, 045204 (2008).
[6] K. Park et al., CLAS Collaboration, Phys. Rev. C **77**, 015208 (2008).
[7] I. G. Aznauryan et al., CLAS Collaboration, Phys. Rev. C **78**, 045209 (2008).
[8] I. G. Aznauryan et al., CLAS Collaboration, Phys. Rev. C **80**, 055203 (2009).
[9] S. Capstick and B. D. Keister, Phys. Rev. D **51**, 3598 (1995).
[10] I. G. Aznauryan, Phys. Rev. C **76**, 025212 (2007).
[11] K. Park et al., CLAS Collaboration, Phys. Rev. C **91**, 045203 (2015).
[12] L. A. Kondratyuk and M. V. Terent'ev, Yad. Fiz., **31**, 1087 (1980).
[13] I. G. Aznauryan, A. S. Bagdasaryan, and N. L. Ter-Isaakyan, Phys. Lett. B **112**, 393 (1982); Yad. Fiz. **36**, 1278 (1982).
[14] I. G. Aznauryan and V. D. Burkert, Phys. Rev. C **85**, 055202 (2012).
[15] I. G. Aznauryan and A. S. Bagdasaryan, Sov. J. Nucl. Phys. **41**, 158 (1985).
[16] B. D. Keister, Phys. Rev. **D49**, 1500 (1994).
[17] I. G. Aznauryan, V. D. Burkert, Prog. Part. Nucl. Phys. **67**, 1 (2012), arXiv:1109.1720, 2011.
[18] F. J. Gilman, M. Kugler, and S. Meshkov, Phys. Rev. D **9**, 715 (1974).
[19] H. J. Melosh, Phys. Rev. D **9**, 1095 (1974).
[20] P. O. Bowman et al., Phys. Rev. D **71**, 054507 (2005).
[21] M.S. Bhagwat et al., Phys. Rev. C **68**, 015203 (2003).
[22] M.S. Bhagwat and P. C. Tandy, AIP. Conf. Proc. **842**, 225 (2006).
[23] R.C.E. Devenish, T.S. Eisenschitz, and J.G. Körner, Phys. Rev. D **14**, 3063 (1976).
[24] H. F. Jones and M. D. Scadron, Ann. Phys. **81**, 1 (1973).
[25] W.W. Ash, Phys. Lett. B **24**, 165 (1967).
[26] A.N. Villano et al., Phys. Rev. C **80**, 035203 (2009).
[27] D. Drechsel, S. Kamalov, and L. Tiator, Eur. Phys. J. A **34**, 69 (2007).
[28] S. Stave et al., Eur. Phys. J. A **30**, 471 (2006).

- [29] N.F. Sparveris et al., Phys. Lett. B **651**, 102 (2007).
- [30] S. Stave et al., Phys. Rev. C **78**, 025209 (2008).
- [31] C. Mertz et al., Phys. Rev. Lett. **86**, 2963 (2001).
- [32] C. Kunz et al., Phys. Lett. B **564**, 21 (2003).
- [33] N.F. Sparveris et al., Phys. Rev. Lett. **94**, 022003 (2005).
- [34] V.V. Frolov et al., Phys. Rev. Lett. **82**, 45 (1999).
- [35] J. J. Kelly et al., Phys. Rev. Lett. **95**, 102001 (2005).
- [36] J. J. Kelly et al., Phys. Rev. C **75**, 025201 (2007).
- [37] T. Sato and T.-S. H. Lee, Phys. Rev. C **63**, 055201 (2001).
- [38] V. D. Burkert and T.-S. H. Lee, Int. J. Mod. Phys. E **13**, 1035 (2004).
- [39] K. Bermuth, D. Drechsel, L. Tiator, and J.B. Seaborn Phys. Rev. D **37**, 89 (1988).
- [40] D.H. Lu, A.W. Thomas, and A.G. Williams, Phys. Rev. C **55**, 3108 (1997).
- [41] A. Faessler, T. Gutsche, B.R. Holstein et al., Phys. Rev. D **74**, 074010 (2006).
- [42] M. K. Jones et al., Phys. Rev. Lett. **84**, 1398 (2000).
- [43] H. R. Grigoryan, T.-S. H. Lee and H. U. Yee, Phys. Rev. D **80**, 055006 (2009).
- [44] K. A. Olive *et al.* [Particle Data Group Collaboration], Chin. Phys. C **38**, 090001 (2014).